

We are IntechOpen, the world's leading publisher of Open Access books Built by scientists, for scientists

6,900

Open access books available

186,000

International authors and editors

200M

Downloads

Our authors are among the

154

Countries delivered to

TOP 1%

most cited scientists

12.2%

Contributors from top 500 universities



WEB OF SCIENCE™

Selection of our books indexed in the Book Citation Index
in Web of Science™ Core Collection (BKCI)

Interested in publishing with us?
Contact book.department@intechopen.com

Numbers displayed above are based on latest data collected.
For more information visit www.intechopen.com



Phase Change Materials for Textile Application

Fabien Salaiin

Abstract

The objective of this chapter is to determine which of the existing PCM families are more suitable for textile thermoregulation while proposing new solutions. Indeed, many of these materials are either limited by their overall enthalpy of phase change or by their thermal window. Thus, it focuses on the study of binary mixing allowing the widening of the temperature range of the phase change and the consolidation of the enthalpy balance by adding chemical species. PCM was microencapsulated to be applied onto textile substrate, before studying the thermal properties.

Keywords: phase change material, textile thermal comfort, paraffin, thermal transition, thermoregulation

1. Introduction

The French textile and clothing industry is facing many difficulties related to competition from countries with low labor costs and relocation. To cope with this, the players in the sector are adapting and diversifying their offer. Traditional industries and markets being the most affected, they are thus moving towards product niches, such as technical and high value-added textile markets, where know-how and innovation play a significant role. New products within particular advanced functionality regarding thermal comfort can help to position themselves in innovative product niches and meet consumer expectations.

The textile structure is involved in maintaining the thermal balance between the heat produced by the body and that given to the external environment. When adequately adapted, it protects the human body from hyper and hypothermia. Its resistance to heat and moisture transfer characterizes it. However, its characteristics depend on external factors such as speed and relative humidity. Thermal insulation in textiles is traditionally made from voluminous composite materials where trapped air plays a key role. Since the late 1980s, a new type of insulation material has appeared on the market, phase change materials (PCMs). Integrated into clothing, they can improve their thermal behavior, regardless of their thickness, guaranteeing a greater freedom of movement for the wearer.

Phase change materials have been used for various applications in thermal energy storage since the 18th century, and many commercial products have been developed to this end. Depending on the field of application, PCMs are selected according to their temperature and phase transition enthalpy. Thus, when their phase change temperatures are relatively low (between -20 and -10°C), these materials are more likely to be used for food storage, while for temperatures

between 2 and 15°C, they are generally used for air conditioning, that is, comfort applications [1]. Higher transition temperatures allow these materials to be used for solar energy storage [2], in agriculture [3], electronic equipment protection [4], or textiles [5–7]. Thermal energy storage by solid-liquid phase change has been the subject of a census by Zalba on more than 150 existing PCMs, 45 of which are commercially available [8].

The thermal properties of phase-change materials allow them to be perceived as the material of choice for thermal insulation of the human body. The possibility of keeping the wearer as long as possible in his thermal comfort zone, and at the same time to reduce the thickness of the garment, is a conceivable objective, taking into account the thermal insulation capacity of textile support containing PCMs. Indeed, these are active during the phase change period and stop when the phase change of all PCMs is complete. This insulating effect is generally referred to as effective thermal insulation. The choice of PCMs to be used is therefore based on the feeling of comfort that the user can feel, regardless of his metabolic activity and external conditions. The effectiveness of PCMs inserted in a textile structure will depend mainly on the temperature differential between the body temperature and that of the surrounding environment. Therefore, a product ideally having a thermal window from 19°C (vasoconstriction temperature) to 37°C should contribute to localized thermal regulation.

The conventional phase change material formulations have some disadvantages related to their chemical structure [9], justifying that they cannot be used without being contained in a capsule or trapped by capillarity in a graphite matrix [10] or chemical gel [11]. Moreover, since these materials can be in a liquid state, they cannot easily be incorporated into a textile carrier without being contained in capsules. Besides, they must be as small as possible in order to facilitate their integration and thermoregulation regarding heat exchange surface, thus helping to compensate for their low thermal conductivity. Regardless of the physical state of the microencapsulated material (solid, liquid, or both), it remains trapped inside. This allows it to be integrated into a textile coating and thus to keep its functionality as long as the coating remains intact.

Microcapsules incorporated in commercial textile composites contain only one active ingredient, usually paraffin. These systems are thus limited by the thermal properties, thermal window, and enthalpy of phase change, of the microencapsulated paraffin. The objective of this work is to develop new materials with improved thermal properties before their incorporation on textile support.

2. Thermal energy storage

The storage of energy in thermal form can be carried out according to three physical principles, that is, (i) sensible heat, (ii) phase change or latent heat, and (iii) thermochemical reactions.

2.1 Storage by sensible heat

Sensible heat storage is undoubtedly common and straightforward, but it is also very inefficient. A material (most often water, stones or thermal oil) is heated to a higher temperature whenever excess heat occurred and cooled when necessary. In general, volume storage capacities remain relatively low. Also, depending on the type of material selected, liquid or solid, the process will be limited in the first case by the chronic tendency to thermal destratification, and in the second by the low thermal conductivity associated with a high porosity rate. In these systems, there

is always a need for a tank and also most often an exchange surface [12]. The cost price of these elements is generally the limiting factor in its economic application. The stored energy (Q in $J\ g^{-1}$) is dependent on both a temperature variation and a function of the mass of material (m) used and its calorific capacity C_p (Eq. (1)). The primary materials used for this type of storage are water, rocks, earth, and ceramics.

$$Q = m \int_{T_{initial}}^{T_{end}} C_p(T) \cdot dT \quad (1)$$

2.2 Storage by chemical reactions or evaporation

Thermal energy storage by chemical reactions is achieved by using the energy released or required during a chemical reaction. The basic principle is as follows (Eq. (2)).



Using the heat provided by the external environment, the AB compound is divided into two components A and B, which can be stored separately. If A is mixed with B, the AB compound is reformed, and the heat is then released. The chemical reactions involved in this process must satisfy the total reversibility of the reaction since the products resulting from the reaction are likely to be separated and can be stored in a solid state and mixed to release heat when energy is required. Adding a catalyst can reduce the reaction temperature, but it is generally high. As a result, research on thermal energy storage by chemical reaction is still in the first stage and cannot be carried out in the short term. Nevertheless, other technologies have developed such as adsorption on activated carbon or zeolite, liquid phase absorption (LiBr), the reaction on chlorides ($MnCl_2$, $NiCl_2$) [13]. Storage systems based on chemical reactions have negligible energy losses, while sensitive heat storage absorbs stored heat from the environment and needs to be isolated from the outside environment [14].

2.3 Storage by latent heat or phase change

Storage by latent heat of fusion is carried out with little or no temperature variation since the phase change of a pure body is isothermal but by phase change of material. The case of alloys is different because melting takes place over a limited temperature range between $T_{solidus}$ and $T_{liquidus}$. Latent heat storage involves a first-order phase transition (enthalpy variation ΔH). When the transition is essential, the material is called PCM (Phase Change Material). These materials are compounds that can store and release thermal energy through their change of state, most often from solid to liquid, but also from solid to solid. When heated, the material takes calories from the external environment and reaches a temperature, T_{tr} , transition temperature, then passing from a phase 1 to a phase 2 by heat absorption. If cooled, the reverse transition occurs at T_{tr} ; the material passes from phase 2 to phase 1 and returns all the previously stored energy to the external environment while remaining at the temperature T_{tr} . The energy involved is the endothermic or exothermic enthalpy variation of the phase change ΔH [15].

Since heat is closely linked to temperature (second principle of thermodynamics), this storage method is more interesting than the first because it allows energy to be stored at a given temperature or a given temperature level. Besides, storage is carried out at a small temperature difference, and it offers the possibility of restoring the stored energy at a constant temperature, at least as long as the solid and liquid phases are in equilibrium. The amounts of stored energy are also higher than when

storing by sensible heat. It should be noted that in practice, not only the latent heat of state change but also the sensible heat of the liquid and the corresponding solid are exploited, which significantly increases the stored energy (Q) (Eq. (3)) [16].

$$Q = m \cdot \int_{T_{\text{initial}}}^{T_{\text{tr}}} C_p(T) \cdot dT + m \cdot \Delta H + m \cdot \int_{T_{\text{tr}}}^{T_{\text{end}}} C_p(T) \cdot dT \quad (3)$$

The phase changes required for this type of storage are first-order transitions. However, only solid-solid and solid-liquid transitions are used [17]. Indeed, the liquid-gas transition is technologically unusable since it leads to too high a variation in volume, and the liquid-liquid transition is vigorously too weak to generate any interest. The use of the solid-solid transition is interesting only in the case where the transition is relatively energetic, that is, for plastic crystal-crystal transitions [18]. The absence of any liquid helps the use of the materials.

3. Properties of phase change materials

The use of latent heat from a phase change material is not in itself a new technique. At the end of the nineteenth century, to overcome the inconvenience of changing hot water bottles too often to heat railway cars, water was replaced by sodium acetate. This salt can store a large amount of heat which it releases entirely after a few hours. While a few patents were filed before 1973, it was not until the first oil shock that many specialized laboratories began research in this field. Taking into account the thermodynamic can only make the choice of good storage material, kinetic, chemical and economic criteria considered essential for the proper functioning of the application in question [19, 20].

3.1 Melting temperature: T_m

It is the first criterion for selecting a product, as it must be appropriate for the application. Its determination by differential calorimetric analysis is relatively easy. However, depending on the origin or purity (and the nature of the impurities) of the materials, it can vary by a few degrees. There are two types of fusion, one ideal called “congruent,” the other called “incongruent.” The ideal fusion is isothermal fusion, where when the material is at the melting temperature, the liquid and solid phases present are in equilibrium and have the same composition. In this case, the change of state occurs reversibly. Thus all the energy stored during melting is fully restored during crystallization, promoting the material’s resistance during the cycles. This type of fusion is generally found in pure substances. The melting can also be incongruous. In this case, two phases are formed beforehand, one liquid and the other solid, and then a fully liquid phase is obtained. Generally, the material decomposes at a temperature below its melting temperature into liquid and crystals. A two-phase mixture with a solid compound of a different composition from the defined compound is obtained in the same way during the cooling. During the cycles, the initial material gradually changes, all the more quickly as variations in density can lead to phase segregation, which accentuates the degradation phenomenon.

3.2 The crystallization temperature/supercooling problem

The crystallization temperature does not necessarily coincide with that of the liquid to solid transition. There is sometimes a slight delay related to the crystallization kinetics which is dependent both on the crystal growth of the material and on nucleation phenomena. This phenomenon also called supercooling, corresponds

to the fact that a body temporarily remains in a liquid state at a temperature below its crystallization point. This is a relatively common phenomenon since even water has a supercooling of a few degrees varying with its impurity level. From a microscopic point of view, supercooling is related to nucleation and the rate of growth of germs. The probability of germ formation is related to the creation of a solid/liquid interface requiring a certain amount of energy. The germ thus created must have a radius more significant than a critical radius, r_c , in order not to be dissolved in the medium. The rate of growth of germs corresponds to the change in the size of the crystal over time. This velocity is zero at the melting point and increases rapidly as the temperature drops to a maximum value. Beyond this value, crystallization will depend mainly on the mobility of the molecules, linked to the viscosity of the medium. Thus, the growth rate decreases with increasing supercooling. Adding a nucleating agent, such as a saline hydrate, stable in the exploited thermal domain and chemically inert towards the storage medium, can eliminate this delay in crystallization. Another solution is to play on the roughness of the container walls to promote nucleation. Supercooling is also related to the mass of the product used; indeed, it decreases considerably with the use of large amounts. Thus, the results obtained by DSC, with masses in the order of mg, must be used with caution. In some cases, supercooling can be considered an asset, since it delays crystallization for a certain period of times.

3.3 The enthalpy of phase change

The enthalpy of fusion corresponds to the energy absorbed by the material during the solid/liquid transition. The liquid/solid transition is achieved by fully restoring this energy. Except in the case of significant supercooling, this is the enthalpy of crystallization. These enthalpies can be determined experimentally by DSC analysis, and like temperatures, differ by a few J g^{-1} depending on the purity and origin of the products. The literature considers that a suitable storage material must have a melting enthalpy, ΔH_m , higher than 180 MJ m^{-3} . Even if some reach 580 MJ m^{-3} , few are those to exceed 350 MJ m^{-3} . A change in volume accompanies a first-order transition, and for most materials, the volume expansion $\Delta V/V$ at fusion is positive except for ice and gallium and its alloys. Depending on the nature of the materials, it can vary from a few percent to 50%, and in particular from 5 to 15% for paraffin.

3.4 Thermal conductivity

Thermal conductivity, λ ($\text{W m}^{-1} \text{K}^{-1}$), is the amount of heat transferred in a unit of time through a material of a surface unit and a unit of thickness when the two opposite sides differ from a unit of temperature. For most materials, thermal conductivity decreases slightly as the temperature rises. Thus, in the liquid state, it is weaker than in the solid state. A high thermal conductivity minimizes temperature differences in the material during melting and crystallization, facilitating heat transfer. Different methods are possible to increase this conductivity, either by inserting fibers or metal matrices, graphite or urea or by increasing the exchange surface.

Thus, the choice of a suitable storage material can only be made by taking into account some of its intrinsic characteristics (melting and crystallization temperatures, enthalpy of phase change, volume expansion and thermal conductivity), but also by knowing its melting behavior and its ability to withstand the thermal cycle, not to mention economic constraints. The last criteria to be taken into account are chemical stability and its non-corrosive aspect to avoid storage problems and material-envelope compatibility.

4. Classification of phase change materials

Among the fusible materials likely to be suitable for heat storage by phase change, there are two main families, that is, (i) organic materials, and (ii) salt hydrates and their eutectics.

4.1 Organic PCMs

Among the organic materials used in latent heat storage, paraffin remains the most commonly used compared to fatty acids, polyethylene glycol (PEG) or benzene derivatives, which nevertheless have good characteristics (congruent fusion, excellent stability, good latent heat, and low corrosion). These fatty acids and their derivatives have excellent thermal characteristics. Nevertheless, their high cost is a barrier to their use. In the rest of this chapter, paraffin is selected due to their high latent heat compared to other potential “choices” are mainly described. Paraffin is linear chain aliphatic hydrocarbons of the general formula C_nH_{2n+2} . Due to their molecular structure and complex structural and thermodynamic behavior, they have been the topic of a many number of studies for more than half a century. These compounds, which are widely distributed in nature in several forms, are found in gasoline and industrial solvents for some carbon atoms (n) between 4 and 10, or in diesel and fuel for $10 \leq n \leq 28$. At $T = 295^\circ K$, the paraffin are gaseous ($1 \leq n \leq 5$), liquid ($5 < n \leq 15$), or solid ($n > 15$) form. On an industrial scale, these compounds are obtained either by cracking and isomerization or by fractional distillation of petroleum.

4.1.1 Chains conformation

The most stable conformation, for which the potential energy is minimal, corresponds to a zigzag arrangement or trans conformation. The symmetry of the molecule depends on the parity of the carbon number. Thus, even n -alkanes have an inversion center while odd-numbered ones have a plane of symmetry perpendicular to the chain. These molecules are likely to have conformational defects, varying according to chain length and temperature. These defects, illustrated in **Figure 1**, result from a sudden increase in the concentration of non-planar conformers among molecules. The first two defects, left terminal type defect and torsion type defect are the most frequent. Conformers with two left bonds are much less numerous, even if their concentration increases near the fusion. The concentration of defects increases significantly with temperature within each crystal phase. It is all the more marked when the temperature is close to the melting point of the materials.

4.1.2 Intermolecular interactions

Since molecules are composed only of carbon and hydrogen atoms, crystal cohesion is ensured through Van der Waals' forces (London, Keesom, Debye), and more specifically London's interactions.

4.1.3 Stacking of molecules

The general laws of compact molecular stacking were established by Kitajgorodskij in 1957 [21]. These laws obey two rules, maximum stacking, and free energy. During the trend towards maximum stacking, molecules minimize their energy by adopting compact arrangements that generate maximum contact. The molecular arrangements observed are those with the highest symmetry compatible with the structure of the molecules. In the case of aliphatic chains, the molecules

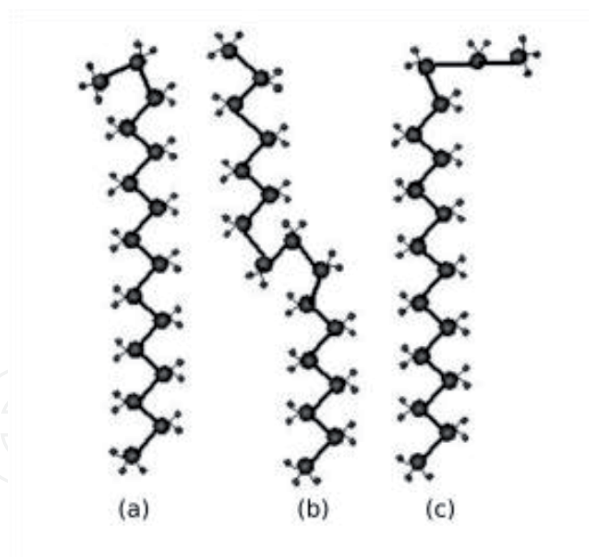


Figure 1.
Conformation defects, (a) left terminal type defect, (b) torsion type defect, and (c) two left connections defect.

are arranged in successive layers, in which the chains are parallel to each other. Therefore, the problem of stacking is at two levels, stacking within a layer and stacking these layers together. During his work, Kitajgorodskij also highlights three types of crystal arrangement: orthorhombic, monoclinic and triclinic.

4.1.4 Structural analysis

The phase changes required for energy storage correspond to first-order transitions. For practical reasons, only solid/solid and solid/liquid transitions can be used. Solid/solid transitions are rarely used because they are too slow, or the amount of energy involved is relatively small. Crystal energy results from two types of intermolecular interactions, those of methylene groups and terminal methyl groups. The values of these forces vary with the length of the chains, leading to differences in the stability of the crystal structure. Thus, n-alkanes crystallize under different structures and are polymorphic, that is, they are likely to undergo one or more solid-solid transitions before melting.

Each structure is part of an elementary mesh whose parameters are defined in the **Figure 2**, where \vec{a} , \vec{b} and \vec{c} , are the basis vectors, and α , β , and γ , the angles between the Oxyz reference axes. The reproduction of this mesh a large number of times allows describing the whole crystal. Each mesh contains one or more molecules and has certain symmetry elements (symmetry axis, inversion center, mirror). A crystallographic group describes each structure:

- orthorhombic structure: $a \neq b \neq c$, $\alpha = \beta = \gamma = 90^\circ$, noted β ;
- triclinic structure: $a \neq b \neq c$, $\alpha \neq \beta \neq \gamma \neq 90^\circ$, noted γ ;
- monoclinic structure: $a \neq b \neq c$, $\alpha = \beta = 90^\circ$, $\beta \neq 90^\circ$, noted δ .

In the aliphatic chains of n-alkanes, each carbon atom is bound to two other carbon atoms and two hydrogen atoms, or one carbon atom and three hydrogen atoms at the end of the chains. The distance between the two carbon atoms is 0.153 nm, and the carbon-carbon binding angle is 114° ; the latter value is higher than that of a perfect tetrahedron ($109^\circ 8'$). The most stable molecular arrangement in the solid state, which corresponds to the minimum in potential energy, is the one where the chains

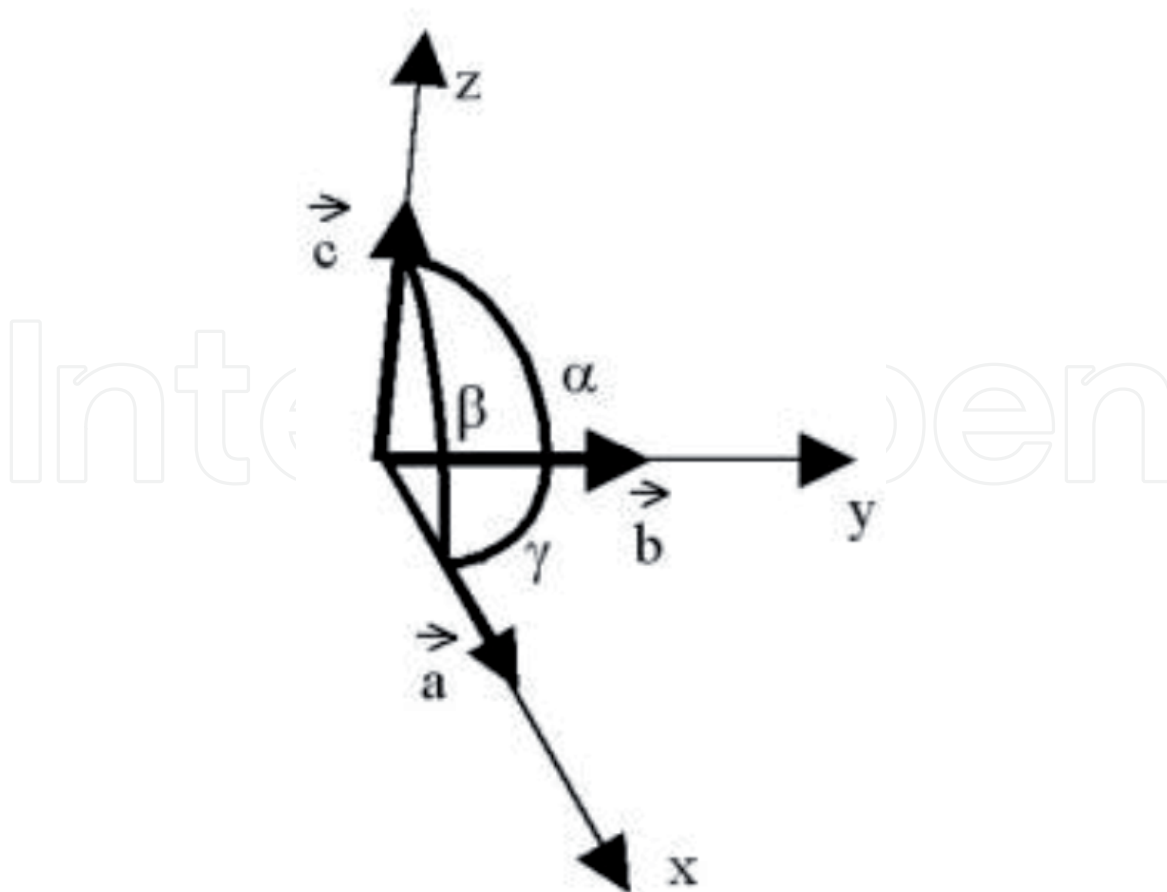


Figure 2.
Lattice constants.

adopt a trans or zigzag conformation. The structure is different according to the parity of the number n of carbon atoms of the n -alkane. Indeed, the steric congestion conditions imply that the $\text{CH}_2\text{—CH}_3$ bonds on either side of the stacking plane are aligned, regardless of the parity of the number of carbon in the n -alkane chain.

4.1.4.1 Low-temperature crystalline structures (ambient temperature)

Historically, the structure of n -alkanes has been discovered by Miller, based on the structure of n -nonacosane ($n\text{-C}_{29}\text{H}_{60}$) [22]. Terminal methyl groups are arranged in planes forming parallel or inclined lamellar surfaces to the axis of the molecular chains. In the solid state, n -paraffin has a much more compact molecular arrangement than in the liquid state. Some paraffin compounds are polymorphic in a defined range of pressure and temperature; they crystallize in different forms. The crystalline phases can be distinguished, in which the chains of carbon atoms are in a perpendicular position concerning the planes of the terminal methyl groups, relative to the orthorhombic structure, noted β_0 ($n\text{-C}_{2p+1}$); and inclined for the planes of the terminal methyl groups, relative to triclinic and monoclinic noted γ_0 ($n\text{-C}_{2p}$) and δ_0 ($n\text{-C}_{2p}$), respectively [23].

The orthorhombic structure β_0 ($n\text{-C}_{2p+1}$) found in odd alkanes ($n \geq 5$) includes four molecules per mesh, two layers of molecules that generate the periodicity in a direction perpendicular to the stacking plane of the chains, with $c = 2 \cdot L$ (L : length of a molecule), and the parallelism of the bonds on either side of the stacking plane of the molecules between the last group CH_2 and the terminal methyl group. The orthorhombic structures of n -alkane mixtures are isomorphic to those of pure n -alkanes. However, they have irregularities at the end of the chain, caused by differences in the length of the molecules.

The series of even n -alkanes between hexane and hexacosane ($6 \leq n \leq 26$) adopts a triclinic structure (γ_0 (n -C_{2p})) with a space group P and some patterns per mesh equal to 1. The series of even n -alkanes ($n > 26$) has a monoclinic structure with two molecules per cell. Besides, it can be noted that the axis of the molecule is inclined to the plane of the terminal methyls. The periodicity is in an oblique direction with regards to the plane by considering the alignment of the links on each side of this plane. Thus, even n -alkanes crystallize in triclinic or monoclinic structures (δ_0 (n -C_{2p})) [23]. **Figure 3** shows this type of molecular arrangement in a triclinic structure along the axis of the chains, as well as the projection on the perpendicular plane.

4.1.4.2 Structure of the high-temperature solid phases (slightly lower than the melting temperature)

High-temperature solid phases called “rotator phases” exist only in a few degrees between the transition temperature in the solid state and the melting temperature. These high-temperature phases maintain an organized structure. In these rotator phases noted, respectively, β -RI and α -RII, the disorder is caused by a 180° rotation of some chains around their axis, which allows them to take a balanced position [24].

The β_0 (n -C_{2p+1}) low-temperature phases of odd n -alkanes undergo a solid state transition accompanied by a significant enthalpic effect that characterizes the appearance of a new orthorhombic phase, noted b. Then, this phase passes into a state called rotator noted β -RI, which has been highlighted by heating only in odd n -paraffin for $9 \leq n \leq 25$. This phase has an orthorhombic structure with the space group Fmmm, where two layers of molecules generate the periodicity in the direction perpendicular to the stacking plane according to the sequence ...ABAB... In the RI state of the β phase, the parameters (a , b) of the mesh continuously change without changing the space group: this causes an evolution as a function of temperature, which certainly reflects a second-order transition.

The rotator phase noted, α -RII, was highlighted in the case of even and odd paraffin for $22 \leq n \leq 26$. The increasing temperature study of the β -RI phase in odd n -alkanes (tricosane and pentacosane) identified the α -RII phase. The transition from the β -RI phase to the α -RII phase occurs when the mesh parameter ratio b/a is equal to $\sqrt{3}$. A change in the stacking sequence accompanies this evolution with the succession ... ABCABC... for the phase α -RII. The transition from the β -RI phase to the α -RII phase is a first-order transition, with a small enthalpy effect.

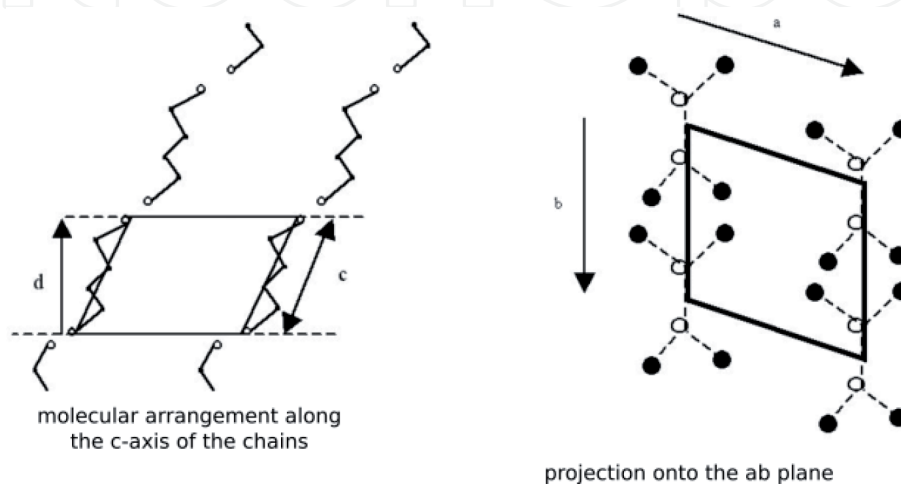


Figure 3.
 Triclinic structure of even n -alkanes.

4.1.5 Thermodynamic analysis

Alkanes are generally characterized by their transition enthalpy (solid 1/solid 2) and melting enthalpy, noted H_{tr} , respectively, and ΔH_m , and by the temperatures at which these phase changes (T_{tr} and T_m) or state occur. We can also look at the global transition enthalpy, noted ΔH_g , which reflects the transition from solid state 1 to liquid (**Figure 4**).

4.1.5.1 Temperature and enthalpy of solid-solid transition

The phase transition temperature changes according to the length of the carbon chain and alternately according to the parity of the molecule. This alternation is because the final crystal structure is different according to the parity of the alkane. Indeed, an odd n-alkane will pass from the orthorhombic phase to the rotator I phase, while the even n-alkane (for $n \geq 20$) will pass from a triclinic or monoclinic phase to a rotator II phase. This alternation is also found on transition enthalpies from $n = 20$; indeed, it appears that the enthalpy is lower for odd n-alkanes than for peers, the difference can be attributed to the evolution for odd ones from the β -RI phase to the α -RII phase (**Figure 5**).

The notation ΔH^* corresponds to the summation of the transition enthalpy (β -RI/ α -RII) and the increase of enthalpy in the β -RI phase. This increase in enthalpy is related to the calorific capacity of this relatively large phase. Thus, this enthalpy gain in the β -RI phase contributes to the even-odd alternation. Nevertheless, solid-solid transitions are generally not very energetic, so they are not always visible in calorimetry.

4.1.5.2 Melting temperature and enthalpy

According to the parity of the n-alkane, and according to the number of carbon atoms it contains, it can be observed an even-odd alternation on the two melting temperature evolutions. This disappears when the structures before fusion of the even and odd n-alkanes are identical, that is, for $n > 20$, as a consequence of the structural difference between the triclinic and rotator I phases.

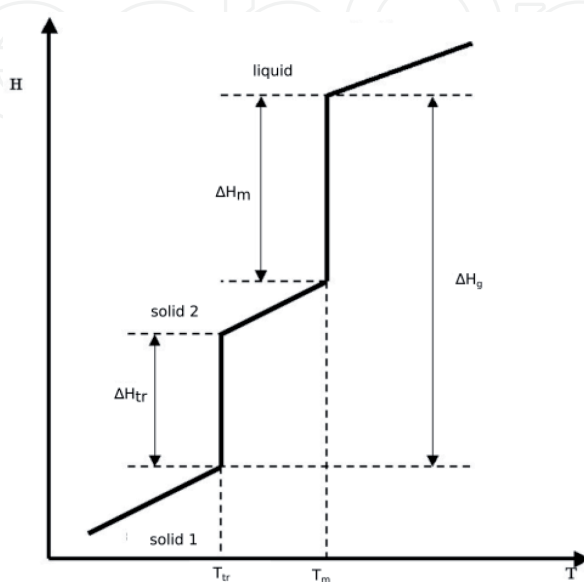


Figure 4.
Evolution of the enthalpy of a pure n-alkane as a function of temperature.

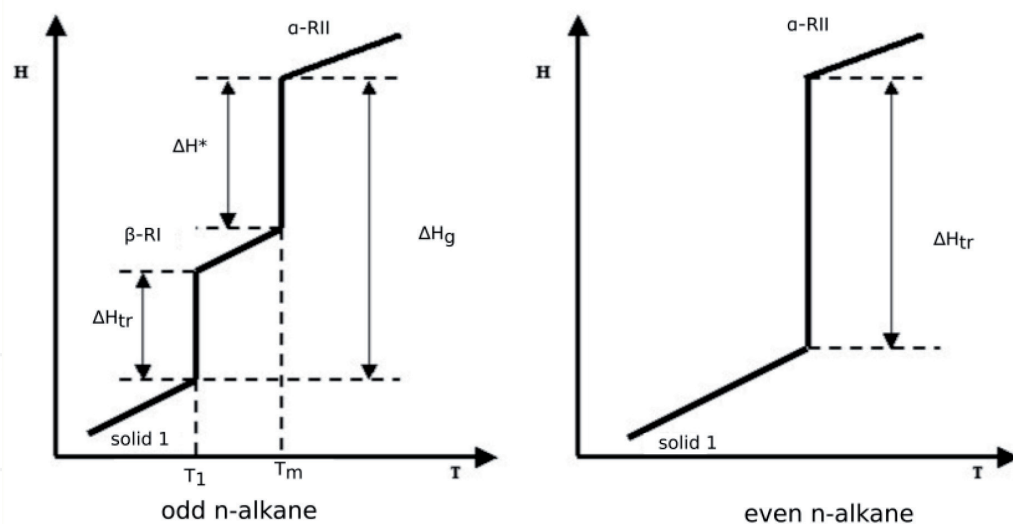


Figure 5.
 Transition enthalpy of odd and even *n*-alkanes.

4.1.5.3 Global enthalpy

The global enthalpy represents the enthalpy balance of all transformations from the solid state to fusion. Its variation is practically linear as a function of the number of carbon atoms [25]. It, therefore, seems that this balance is independent of the nature of the low-temperature phase and the parity of the *n*-alkane.

4.1.6 Improvement of thermal conductivity

Much research has attempted to compensate for the poor thermal conductivity of paraffin by adding fins or expanded metal to the material or by dispersing it in a porous conductive material such as natural expanded graphite [26]. This method makes it possible to obtain composites with high thermal conductivity, high paraffin mass content (65–95%) trapped by capillarity [27]. A more common solution is to divide paraffin by volume by encapsulating it in PE spheres or by dispersing it as an emulsion in water. However, such a solution has the effect of considerably reducing (50%) the effective volumetric heat capacity of the process. In other words, its power is improved, but it takes up twice as much space.

4.1.7 Binary systems of *n*-alkanes

By combining alkanes in pairs, it is possible to develop systems of various structural types, some of which have very interesting thermal characteristics for energy storage [28]. The study of the behavior of binary mixtures of *n*-alkanes through phase diagrams or phase equilibrium has generated growing interest in the design of latent heat storage materials since it allows the prediction of the system's behavior during phase changes. Nevertheless, this behavior is governed by some general rules of thermodynamics on the possibility of forming solid solutions.

4.1.7.1 Gibbs rule

The solid solution of two *n*-alkanes is favored if the Gibbs free energy of the mixed crystal is lower than that of each of the pure constituents; otherwise, there is no miscibility in the solid state, but a eutectic.

4.1.7.2 Symmetry rule

Two n-alkanes are only miscible if they have the same crystal structure. This prerequisite, which was first formulated by Kitajgorodskij, is necessary but not sufficient [21], concerns n-alkanes of neighboring chain lengths.

4.1.7.3 Kravchenko rule

Kravchenko defines a criterion that predicts the mutual solid state solubility of two n-alkanes in the form (Eq. (4)) [29]:

$$\tau = \frac{n - n'}{n} \quad (4)$$

With n and n' denoting the number of carbon atoms contained in each molecule. Thus, the total solubility is obtained for $\tau < 0.06$, it is partial when $0.06 < \tau < 0.15$, and almost null for $\tau > 0.15$.

However, the latter rule is insufficient since the symmetry rule implies that n-alkanes below C_{36} whose chain length differs from one unit cannot have total solubility since they are not isomorphic. Thus, many authors present phase diagrams in the literature where this rule is not respected. Also, Agafonov et al. [30], and He and Setterwall [31], also reported that the mixture of two isomorphic components in the solid state forms a continuous solid solution.

Therefore, synthetic paraffin has many advantages (no or low subcooling, perfect thermal reversibility) but remain relatively expensive and have a very low thermal conductivity ($\lambda = 0.24 \text{ W m}^{-1} \text{ K}^{-1}$), which inhibits phase change kinetics and reduces the available powers accordingly. Their latent heat and density increase as the number of carbon atoms increases from C_1 to C_{40} and stabilizes around 280 J g^{-1} and 820 J m^3 , respectively. The melting temperature also varies very gradually from 91 to 388°K depending on the number of carbon atoms, which potentially makes the use of this family of materials very flexible.

4.2 Inorganic PCMs

Inorganic PCMs, and more specifically saline hydrates, represent an interesting alternative to paraffin because of their low cost, high storage density (between 250 and 400 MJ m^{-3}), and relatively good thermal conductivity [32]. However, the main problem encountered when using these materials is phase segregation during melting [33]. Indeed, many of them have an incongruous fusion, making the system irreversible.

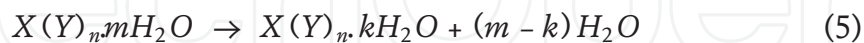
4.2.1 Physico-chemical properties of materials

The realization of energy storage by latent heat is related to the physico-chemical properties of the materials used, that is, (i) subcooling, (ii) crystallization rate, (ii) and the melting. A rapid rate of crystallization is generally required to allow the energy absorbed by the material to be released within a reasonable time. However, latent heat storage systems, because of their operation under a low-temperature difference, require a low crystallization rate. Acceleration of crystallization kinetics can be achieved by introducing solvents with high polarity and a high dielectric constant in order to improve ion mobility. Hydrated salt can be classified according to their type of melting into four categories, that is, (i) congruent melting, (ii) semi-congruent melting hydrates, (iii) non-congruent melting, and

(iv) eutectics [34]. Of these four types of transitions, only two correspond to perfectly reversible transitions: congruent melting and eutectic. The other two are characterized by the transition from a solid single-phase state to a liquid/solid two-phase state. The degree of incongruous melting varies according to the hydrates considered. Nevertheless, some hydrates do not show incongruent fusion, but their cost is relatively high.

4.2.2 Solid-liquid balance

During its fusion, the salt, noted $X(Y)_n \cdot mH_2O$, is likely to undergo one of the following two reactions (Eqs. (5) and (6)).



Hydrated salt tends to separate into two phases, no longer maintaining the salt/water ratio in suitable proportions. A salt-rich liquid (denser) tends to accumulate at the bottom of the container, and a water-rich salt solution floats over the whole. When repeating fusion/crystallization cycles, less and less salt and water can come together and react to form a hydrate with the desired melting temperature. Part of the solid cannot be melted, and part of the liquid cannot be crystallized. The effect is a gradual loss of phase change enthalpy and latent heat storage capacity [35]. The most effective method to overcome this problem remains the suspension or agitation of the system. Suspension requires the introduction of clay or the formation of a gel that traps the hydrate so that when it crystallizes, salt and water are in contact to allow the system to recombine. The dimensions of the storage container can also be adjusted by minimizing them to limit phase separation.

4.2.3 Anhydrous rearrangement

The effectiveness of these materials is related to the amount of water and salt that can react to form the hydrated form. In the case of sodium sulfate, it appears that the salt settles very quickly, and rearranges [36]. As a result, it only partially hydrates, generating a low storage material. The addition of a continuous quantity of water up to the crystallization point makes it possible to overcome this problem. Nevertheless, shaking the system is strongly required to optimize the formulation of the PCM.

Therefore, among inorganic compounds, only saline hydrates and their eutectics have acceptable properties, including high latent heat and relatively low prices. Nevertheless, these materials have some limitations for latent heat energy storage including subcooling and their tendency to melt incongruently. This phenomenon is all the more embarrassing as it leads to the non-reversibility of the change of state. This problem can be eliminated by adding a clay-based gelling mixture that inhibits the settling effect of the lower hydrate [37]. Reversibility is thus restored within a reasonable time. The final limitation for these compounds is their low crystallization rate, which limits the thermal storage capacity. Some solvents or additives with high polarity and high dielectric constant accelerate the kinetics [38]. Indeed, better mobility of ions and therefore a high dielectric constant leads to a decrease in liquid-solid interfacial energies.

The performance of a latent heat storage system is based on the thermal properties of the compounds selected according to their melting and crystallization temperature, which must be in adequacy with the intended application, but also the enthalpy of phase change, and their stability during their implementation. The

choice of one family over another is generally a function of the application and the initial cost of the products.

5. Formulation for textile thermoregulation

In recent years, phase-change materials have generated particular interest in thermal energy storage. The advantage of using latent heat storage lies in the possibility of optimizing the thermal windows of use (or “activation”) by the judicious choice of materials based on both temperatures and phase transformation enthalpies. The action of PCMs incorporated in textile composites is “temporary” or “transient,” that is, it is effective as a barrier to thermal energy until all latent heat stabilizing the exchange temperature is absorbed or released during the phase change of the material. Thus, by choosing a PCM formulation adapted to exchanges, thermal energy can be stored or released, and can effectively be “recharged” by heat or cold source. Among the existing PCMs, we have chosen to work with paraffin, or n-alkanes, which are ideal candidates for latent heat thermal energy storage due to their thermal characteristics with phase change enthalpies in the order of 200 J g^{-1} and phase transition temperatures varying according to their number of carbon atoms in the molecules (**Table 1**).

The objective of this part is first to identify potential candidates from among all present n-alkanes likely to be suitable for textile thermoregulation, then to develop a formulation by binary mixing, by determining thermo-physical properties and by energy characterizations by differential enthalpy analyses.

5.1 Choice of materials: enthalpy analysis of pure substances

The thermal characteristics of the selected n-alkanes (n-hexadecane, n-heptadecane, n-octadecane, n-nonadecane, and n-eicosane) were studied by differential calorimetry using the computer-controlled TA Instrument type DSC 2920 apparatus using the TA Advantage control software. The analyses are carried out under nitrogen flow with a flow rate of 50 ml min^{-1} . The samples, with a mass of about $4.0 \pm 0.1 \text{ mg}$, are placed in an aluminum crucible, closed by a cover on which two holes have been made to ensure the chemical inertia of the medium.

5.1.1 The even n-alkanes

The thermograms of n-hexadecane (**Figure 6**) and octadecane (**Figure 7**), during a fusion-crystallization cycle, are characterized by an endothermic peak during the heating and transition from triclinic to liquid structure and an exothermic peak during the cooling (liquid to triclinic).

The enthalpies and phase change temperatures measured are in accordance with those found in the literature. In both cases, it is also observed that the melting peak is always preceded by a slight deviation from the baseline a few degrees before the melting, due to the existence of pre-melting phenomena.

The case of n-eicosane is different. Although the 2°C min^{-1} cycles initially allowed us to measure enthalpies and phase change temperatures similar to those cited in the tables, the exothermic peak raised some questions. Indeed, the thermogram (**Figure 8(a)**) shows that this compound does not have any polymorphism during the temperature rise while the cooling presents a cluster of peaks that deconvolves into two distinct peaks during a cycle at $0.5^\circ\text{C min}^{-1}$ (**Figure 8(b)**). We observe the liquid/a-Rotator II/triclinic transitions. The existence of this

| n-alkane | Carbone atoms | Melting point (°C) |
|---------------|---------------|--------------------|
| n-octacosane | 28 | 61.4 |
| n-heptacosane | 27 | 59.0 |
| n-hexacosane | 26 | 56.4 |
| n-pentacosane | 25 | 53.7 |
| n-tetracosane | 24 | 50.9 |
| n-tricosane | 23 | 47.6 |
| n-docosane | 22 | 44.4 |
| n-heneicosane | 21 | 40.5 |
| n-eicosane | 20 | 36.8 |
| n-nonadecane | 19 | 32.1 |
| n-octadecane | 18 | 28.2 |
| n-heptadecane | 17 | 22.0 |
| n-hexadecane | 16 | 18.2 |
| n-pentadecane | 15 | 10.0 |
| n-tetradecane | 14 | 5.9 |
| n-tridecane | 13 | −5.5 |

Table 1.
Change in the melting temperature of *n*-alkanes as a function of the number of carbon atoms.

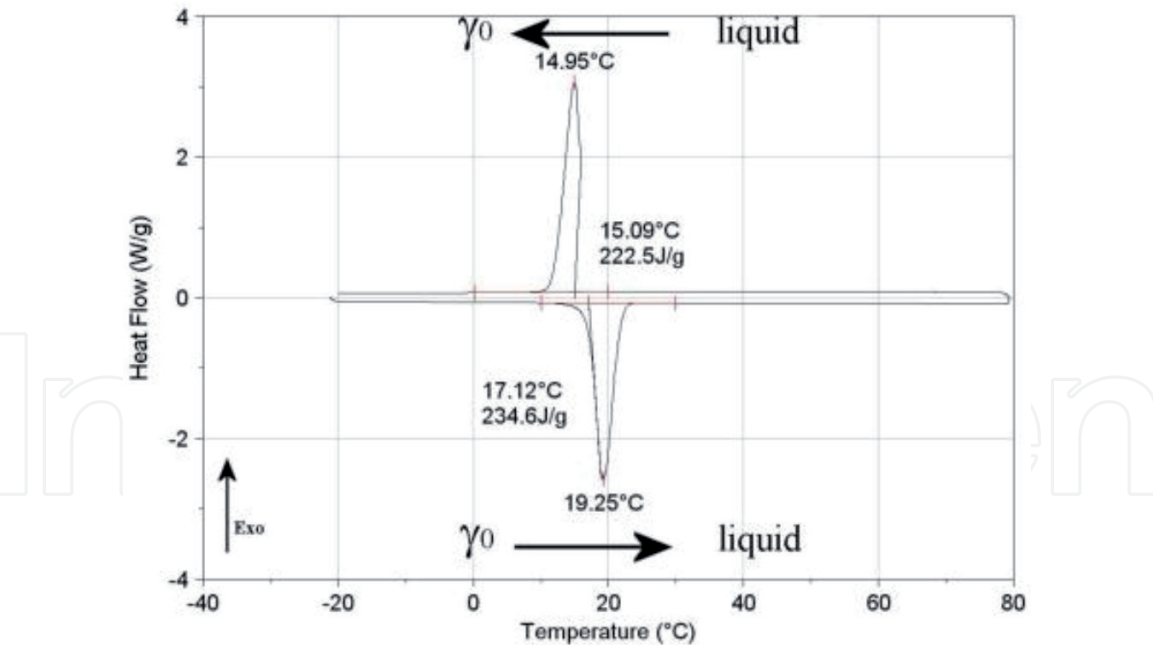


Figure 6.
Heating and cooling curves of *n*-hexadecane (N_2 , 2°C min^{-1}).

rotating structure varies between 30 and 34°C, depending on the number of cycles imposed on the sample.

During his work, Espeau also noticed this type of variation for different samples analyzed under the same conditions [39]. The existence of this phase was not observed when the temperature increased. To observe it, it would have been necessary to raise the temperature after crystallization and before the solid-solid phase

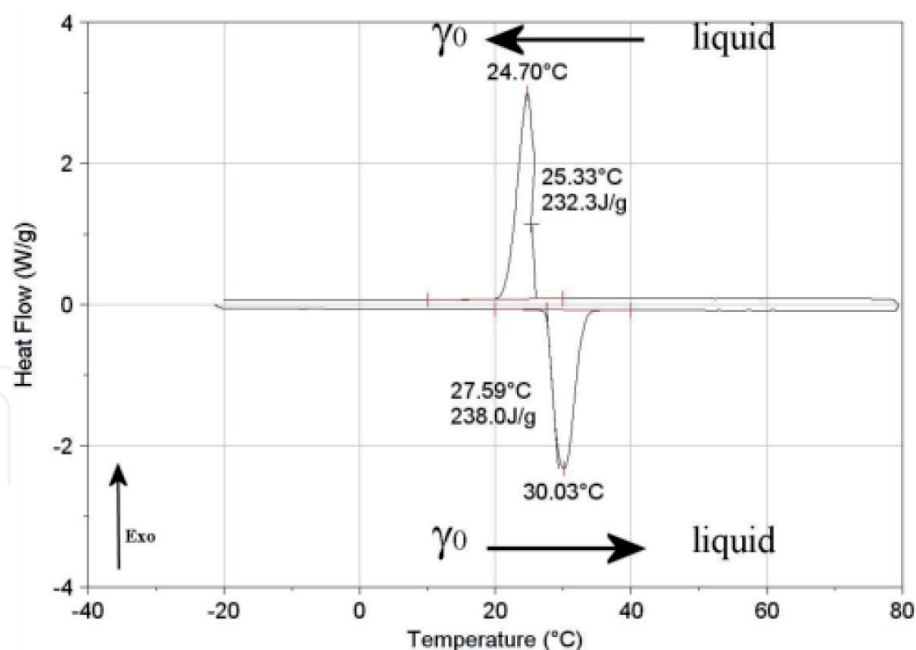


Figure 7.
Heating and cooling curves of *n*-octadecane (N_2 , 2°C min^{-1}).

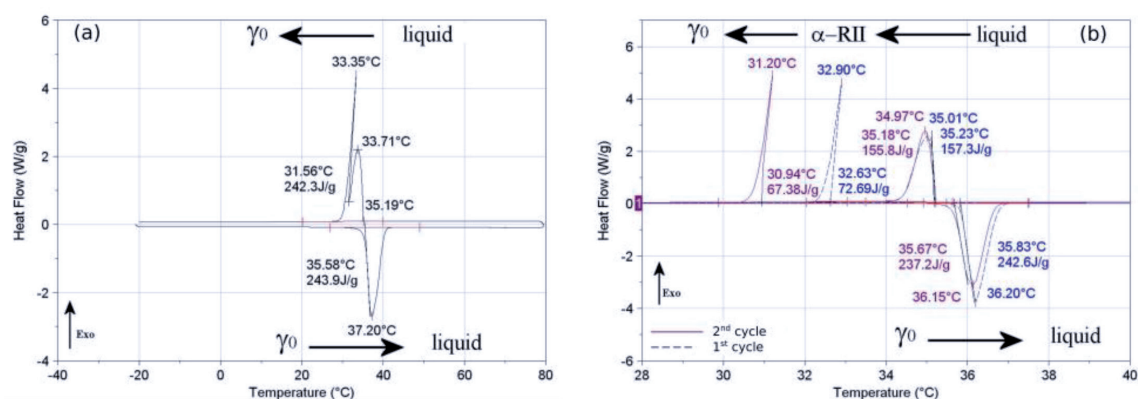


Figure 8.
Heating and cooling curves of *n*-eicosane (N_2 , 2°C min^{-1} (a) and $0.5^\circ\text{C min}^{-1}$ (b)).

change. The solid-solid transition enthalpy is slightly lower than that measured by Espeau. This difference can be blamed on the measuring instrument. Indeed, it was noted that whatever the temperature ramp imposed for this type of paraffin, the DSC did not keep its set point during the phase change. This phenomenon can be minimized by reducing the mass of the sample, but can still be observed for a ramp of $0.5^\circ\text{C min}^{-1}$ and a mass of about 1 mg.

5.1.2 The odd *n*-alkanes

The thermograms presented in the **Figures 9** and **10** show the existence of two endothermic phenomena related to the solid phase transition of the orthorhombic structure, β_0 , to the rotator I phase, and to the solid-liquid transition by the rotator I/liquid fusion. Similarly, the temperature decrease is marked by the presence of two exothermic peaks corresponding, respectively, to the liquid/rotator phase change I and the solid/solid rotator transition I/ β_0 . The temperatures and enthalpies of phase changes and solid/solid transitions are of the same order of magnitude as those measured by Espeau but slightly lower than those of Barbillon's work [40].

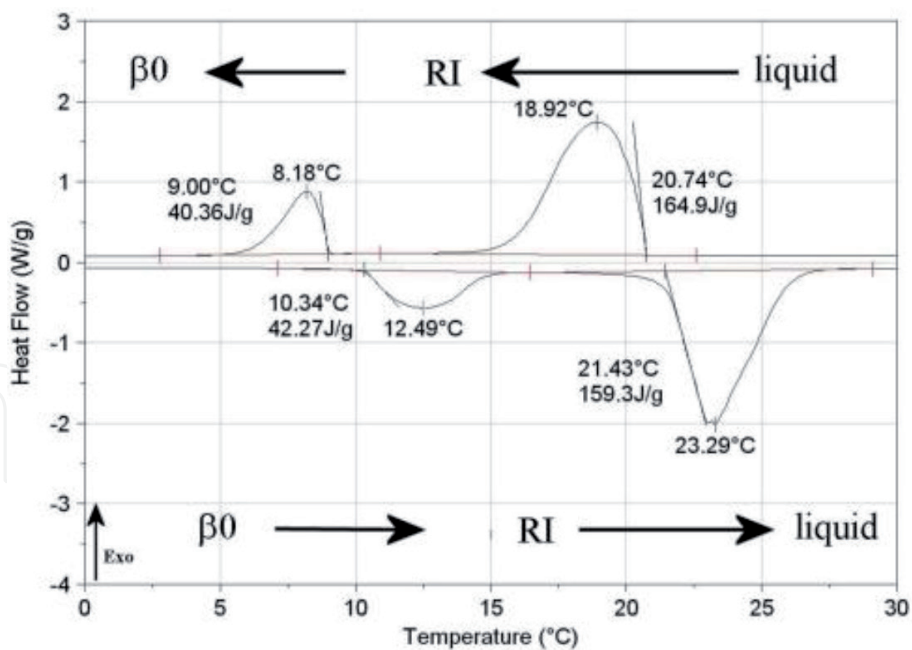


Figure 9.
Heating and cooling curves of *n*-heptadecane (N_2 , 2°C min^{-1}).

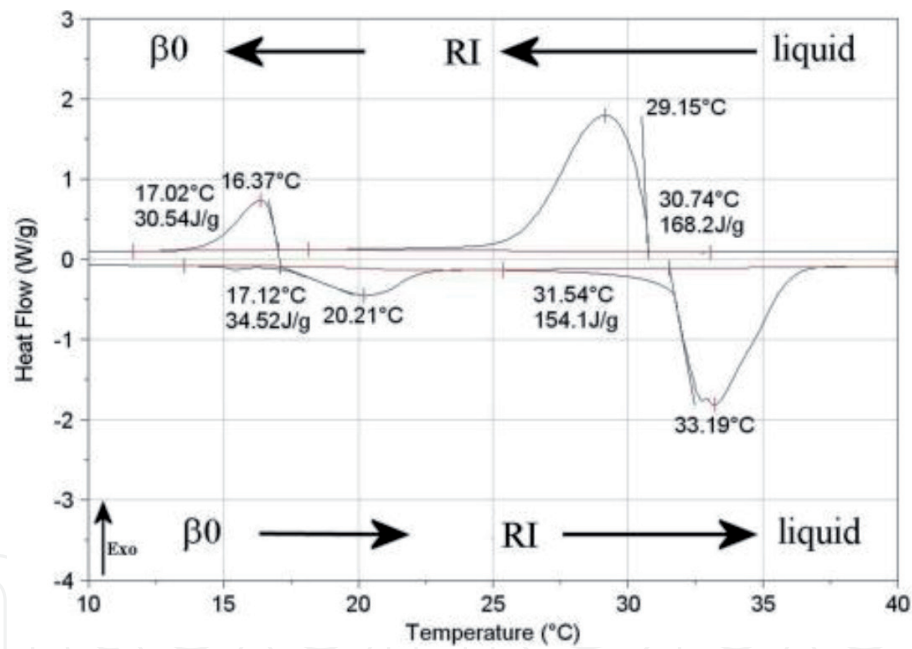


Figure 10.
Heating and cooling curves of *n*-nonadecane (N_2 , 2°C min^{-1}).

6. Thermal span adjustment of binary mixture C_{16}/C_{20}

The study of simple compound made it possible to thermally characterize the different kinds of paraffin likely to be suitable for textile thermoregulation. However, none of them have a sufficiently wide thermal span between 19 and 30°C. Odd *n*-alkanes appear to be of little interest given the existence of a solid/solid transition with low energy and a lower enthalpy of solid/liquid phase change than for even *n*-alkanes. Also, their cost is four times higher than that of even *n*-alkanes, justifying the fact that these two compounds do not appear to be ideal candidates for this research. Of the remaining three *n*-alkanes, we focused on the

binary mixture C_{16}/C_{20} , due to their respective melting temperatures on either side of those required for the application. Also, the objective is to obtain a succession of phase transitions, which can be induced by the superposition of crystals of different sizes and the partial miscibility of n-alkanes. It is hoped that all transitions will be

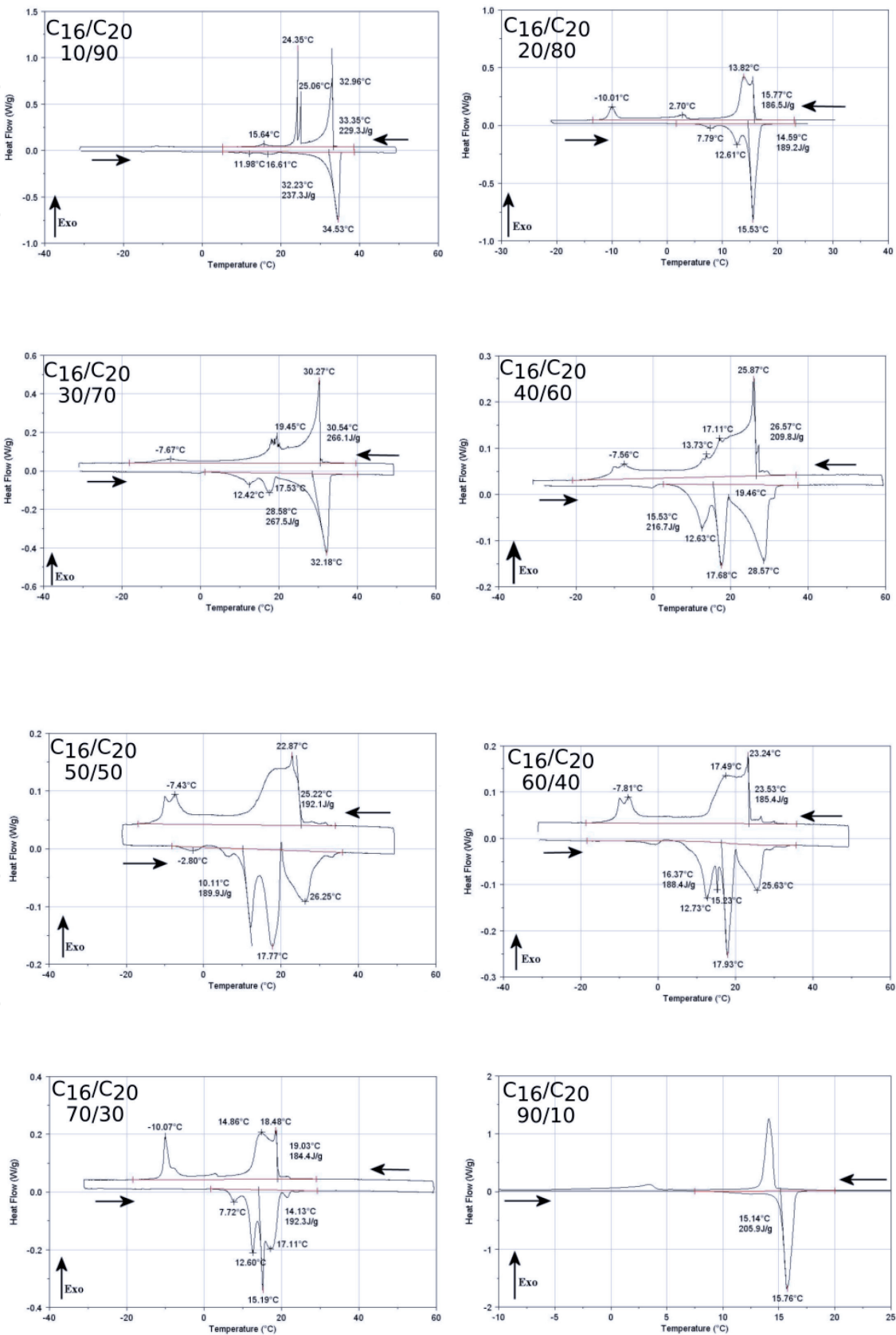


Figure 11.
Heating and cooling curves of C_{16}/C_{20} binary mixture at various ratio.

contained within a single, relatively large peak. The binary diagrams C_{16}/C_{18} and C_{18}/C_{20} presented in Métivaud's work show that solid/solid and solid/liquid transitions occur over relatively narrow and distinct temperature ranges and are therefore not suitable for textile application [41–43].

The enthalpy characterization of the C_{16}/C_{20} mixture in different proportions was performed with 3 mg samples and a temperature ramp of $0.5^{\circ}\text{C}/\text{min}$, allowing the peaks for the different transitions to be dissociated. All the thermograms relating to this mixture are presented in **Figure 11**. The superposition of the endotherms shows that when one of the compounds is in the majority in the mixture, the thermal phase transition windows are narrow and tend towards those of the alkane fusion in a higher proportion. On the other hand, for mass fractions between 0.3 and 0.7, there is an expansion of the endotherms between 0 and 35°C , implying the appearance of new solid/solid transitions within the material during the temperature rise.

The measurement of enthalpies shows that they vary between those of pure substances and 190 J g^{-1} , except in the particular case of mixing in a 30/70 ratio (hexadecane/eicosane). Thus, the widening of the thermal window is accompanied by a decrease of about 20% in the total enthalpy of phase changes. This “loss” is related to the increase in the number of solid/solid transitions that are less energetic than solid/liquid transitions. We finally chose the 50/50 mixture, which allowed us to load the material over a larger thermal window observed from 3 to 32°C for enthalpy of 190 J g^{-1} .

The binary mixture of the two kinds of paraffin disrupts the cohesion of the crystal, which results in a succession of solid/solid transitions inducing the widening of the thermal window and the decrease of the overall enthalpy. Based on this hypothesis, we focused on the introduction into the mixture of a “soluble” charge in any proportion whatsoever in hexadecane and eicosane. We chose tetraethyl orthosilicate. The measurements of the overall enthalpies of the mixture as a function of the charge ratio show that the latter makes it possible to increase the energy balance to values comparable to those of pure substances, then from 4% in weight, the enthalpy decreases until reaching its basic level at 20% (**Figure 12**).

Among the five n-alkanes selected, based on their melting temperatures, the even n-alkanes have a higher enthalpy of phase change and are less expensive. The binary mixing of n-hexadecane with n-eicosane allows the thermal window to widen with a decrease in phase transition enthalpies. The addition of a “miscible” charge in the pre-selected mixture consolidates the energy balance without modifying the thermal span.

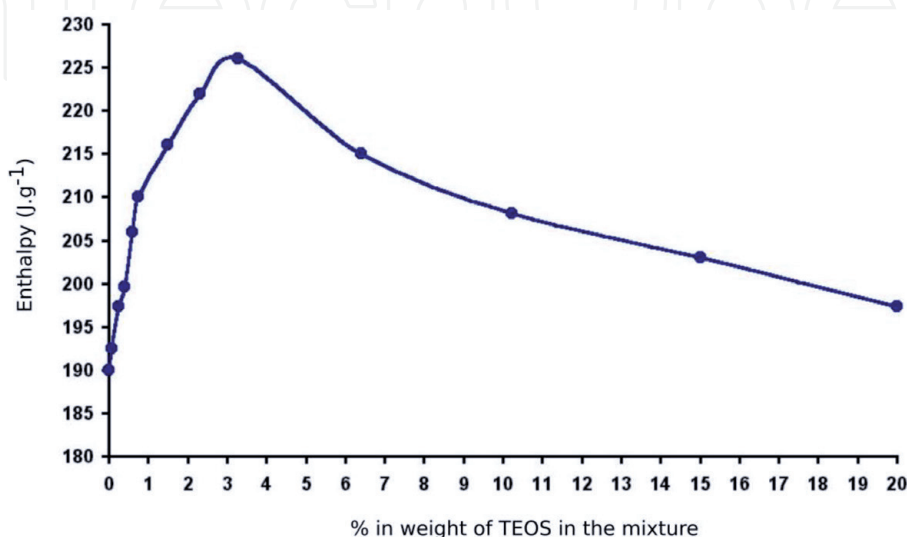


Figure 12.
 Enthalpy variation vs. TEOS content.

7. Textile application

Since these materials may be in a liquid state, they cannot be easily incorporated into a textile carrier without being contained in capsules, which must be as small as possible to facilitate thermoregulation. Microencapsulation techniques may vary depending on the constitution of the membrane. Nevertheless, they all start with an oil-in-water or water-in-oil emulsion step depending on the solubility of the principle to be encapsulated in one or the other of these phases. In our case, the dispersion of paraffin in water is done by means of a rotor-stator. Microcapsule synthesis is continued by adding a melamine-formaldehyde-based prepolymer and reducing the pH for polycondensation of resin chains around PCM droplets. The formation of the aminoplast shell allows the active principle to be correctly isolated from the external environment and prevents any diffusion, and provides an interesting mechanical and thermal resistance for application on textiles. This in situ polymerization allows the production of microcapsules with a relatively narrow and controlled granulometry, by controlling the different physico-chemical parameters governing the emulsion stages (shear, pH, temperature, surfactants, interfacial tension...) and membrane growth [5, 6, 44].

Regardless of the physical state of the material inside these microcapsules (solid, liquid, or both), it remains trapped inside. This allows it to be integrated into a textile coating or incorporated into different artificial fibre compounds and can be effective as long as the coating or fibres themselves remain intact. For the application of these materials on textiles by bath impregnation, we used a thermodynamic approach to wetting to characterize the textile/binders/microcapsules interfaces. Thus, the comparison of the components of the surface energy of the polyurethane binders with those of the resins forming the membrane of the microcapsules, allowed us to optimize our formulation, before validating it by the ISO 6330 standard.

A 100% cotton fabric (566 dtex warp and 564 dtex weft yarns at densities of 26 ends/cm \times 16 picks/cm, weighing 270 g m⁻², thickness of 0.50 mm), labelled COT, a 100% polyester fabric (345 dtex warp and 290 dtex weft yarns at densities of 18 ends/cm \times ~7 picks cm⁻¹, weighing 178 g m⁻², thickness of 0.22 mm) (PES), and a PES nonwoven (155 g m⁻²) were chosen as the textile specimens (**Table 2**).

The thermal resistance to exchanges is expressed in m² °C W⁻¹. The clothing isolation unit used is the clo, defined as the isolation of clothing necessary to maintain the thermal balance of a resting subject exposed to calm air and a temperature of 21°C. In practice, 1 clo corresponds to the isolation provided by classic streetwear and common underwear.

The heat transfer resistance for a sample, including the thin layer of air between the textile and the module, is calculated according to the Eq. (7).

$$R_t = \frac{(T_{sk} - T_a)A}{H} \quad (7)$$

where R_t is the thermal resistance in m² °C W⁻¹, A the surface area in m², T_{sk} the temperature (35°C), T_a the ambient temperature (°C) and H the heat flow in W.

The coating generates a modification of the surface and the context of the support, thus modifying the transfer of heat flows. Nevertheless, the evolution of R_t as a function of the mass deposited shows, and in particular in the case of cotton, that a low coating makes the textile less insulating and that a minimum quantity is required to reach the level of the reference sample. This characteristic is closely linked to the presence of an uniform or uneven deposition on the surface that modifies the contribution of air, by substituting free volumes with polymer volumes. Indeed, a low rate, as is the case for the COT1/2-(17) and PES1/2-(35) samples, does

| Sample label | Ta = 21°C | | Tb = 32°C | Weight deposited (g m ⁻²) |
|-------------------|---|----------|---|---------------------------------------|
| | Rt (m ² °C W ⁻¹) | Rt (clo) | Rt (m ² °C W ⁻¹) | |
| Pristine cotton | 0.070 | 0.451 | 0.094 | 0 |
| COT1/2-(17) | 0.068 | 0.438 | 0.085 | 17 |
| COT1/2-(39) | 0.069 | 0.445 | 0.090 | 39 |
| Pristine PET | 0.071 | 0.460 | 0.098 | 0 |
| PES1/2-(35) | 0.068 | 0.443 | 0.096 | 35 |
| PES1/2-(50) | 0.074 | 0.480 | 0.099 | 50 |
| PES1/2-(101) | 0.068 | 0.437 | 0.105 | 101 |
| Pristine nonwoven | 0.093 | 0.604 | 0.093 | 0 |
| NT1/2-(65) | 0.094 | 0.608 | 0.146 | 65 |
| NT1/2-(95) | 0.089 | 0.577 | 0.113 | 95 |

Table 2.
Thermal resistance of the obtained textile samples determined at 21 and 32°C.

not allow a uniform film to be obtained. Thus, there is a competitive phenomenon between the modification of factors influencing convection, such as the volume, porosity, and geometry of the textile, decreasing the amount of air within the material, and the action of microcapsules containing phase change materials. When the structure is uniformly covered, which is the case for PES1/2-(50) and PES1/2-(101), and that the film is sufficiently impermeable to air, thus to the renewal of the microclimate through the textile, the thermal resistance of the samples is higher than that of the reference.

The choice of a process for implementing microcapsules of PCMs on textile support remains a crucial step in the implementation of thermoregulatory structures. The functionalization of nonwoven is an excellent example since it is the structure with the highest % of free volume, its construction is random, and it is the thickest, that is, as much of factors that make the inherent insulating power of air predominate. Thus, whatever the mass deposited, its thermal resistance remains lower than that of the original textile at 21°C. The full bath coating with squeezing not only modifies the porosity of the material but also its compactness, making it difficult to exploit the results.

Therefore, the most suitable process for nonwovens is the lick roller coating. However, the thermal properties of the samples are worse than the reference but higher than those of NT1/2-(95). When analyzing their samples of foam-coated nonwovens and PCM microcapsules, Shim et al. [45] also, reveal that the thermal resistance of their materials reduced to one unit thickness is lower for structures containing PCMs than without.

The evaluation of the thermal behavior of textile structures has shown that it is linked to the deposition process used, the mass deposited, the nature and the context of the textile support used. The modification of the textile fabric structure during impregnations has a significant influence on the thermal behavior of textile composites. Indeed, small deposited masses generate a lower thermal resistance than the reference sample due to the decrease in air permeability. Also, the temperature gradient within the structure influences the loading of MPCMs. Thus, surface impregnation allows a higher rate of active ingredient to be activated over a wider thermal window. Because of the results, it is necessary to deposit a certain amount of MPCMs to compensate for the thermal insulation lost when the context

is modified. Indeed, this modification during the coating with the binder and microcapsules reduces the porosity of the material. Thus, from higher mass deposits, the thermoregulatory effect of MPCMs is perceptible and allows to improve thermoregulation. Nevertheless, the optimization of the binder/microcapsule ratio is essential to more explicitly quantify the role played by these two elements in the perceived effect.

8. Conclusion

The use of PCMs is based on the encapsulation by an aminoplast membrane of a binary mixture of paraffin. Thus, as a first step, we determined the PCM adapted to our study, namely a binary formulation of n-hexadecane/n-eicosane (50/50), allowing the thermal window to be extended over a temperature range of -10 to 30°C with an overall phase change enthalpy of 190 J g^{-1} , that is, 20% lower than that of n-alkanes taken separately. The introduction of TEOS at 4% has made it possible to consolidate the energy balance at 230 J g^{-1} . In a second step, during the microencapsulation of this formulation with an aminoplast resin on a laboratory scale, we obtained microcapsules with an average diameter between 1 and $5\text{ }\mu\text{m}$. We observed that the final particle size of the particles obtained was very dependent on the particle size resulting from the emulsification step.


The thermal characterization using a hot guarded plate showed the importance of the textile context during heat transfers. Thus, a minimum amount of binder and microcapsules deposited mass is required to compensate for the change in this context during the implementation step. This quantity is 20 g m^{-2} for binders and 40 g m^{-2} for microcapsules. Also, the responses to thermal variation depend on the mass deposited.

Author details

Fabien Salaün
ENSAIT-GEMTEX, Roubaix, France

*Address all correspondence to: fabien.salaun@ensait.fr

IntechOpen

© 2019 The Author(s). Licensee IntechOpen. This chapter is distributed under the terms of the Creative Commons Attribution License (<http://creativecommons.org/licenses/by/3.0>), which permits unrestricted use, distribution, and reproduction in any medium, provided the original work is properly cited. 

References

- [1] Cabeza LF, Mehling H, Hiebler S, Ziegler F. Heat transfer enhancement in water when used as PCM in thermal energy storage. *Applied Thermal Engineering*. 2002;22(10):1141-1151. DOI: 10.1016/S1359-4311(02)00035-2
- [2] Hawlader MNA, Uddin MS, Zhu HJ. Preparation and evaluation of a novel solar storage material: Microencapsulated paraffin. *International Journal of Science Education*. 2000;20(4):227-238. DOI: 10.1080/01425910008914357
- [3] Marinković M, Nikolić R, Savović J, Gadžurić S, Zsigrai I. Thermochromic complex compounds in phase change materials: Possible application in an agricultural greenhouse. *Solar Energy Materials and Solar Cells*. 1998;51(3):401-411. DOI: 10.1016/S0927-0248(97)00259-6
- [4] Baby R, Balaji C. Experimental investigations on phase change material based finned heat sinks for electronic equipment cooling. *International Journal of Heat and Mass Transfer*. 2012;55(5-6):1642-1649. DOI: 10.1016/j.ijheatmasstransfer.2011.11.020
- [5] Salaün F, Devaux E, Bourbigot S, Rumeau P. Application of contact angle measurement to the manufacture of textiles containing microcapsules. *Textile Research Journal*. 2009;79(13):1202-1212. DOI: 10.1177/0040517508100724
- [6] Salaün F, Devaux E, Bourbigot S, Rumeau P. Thermoregulating response of cotton fabric containing microencapsulated phase change materials. *Thermochimica Acta*. 2010;506(1-2):82-93. DOI: 10.1016/j.tca.2010.04.020
- [7] Salaün F. Microencapsulation technology for smart textile coatings. In: Hu J, editor. *Active Coatings for Smart Textiles*. Cambridge: Woodhead Publishing; 2016. pp. 179-220
- [8] Zalba B, Marín JM, Cabeza LF, Mehling H. Review on thermal energy storage with phase change: Materials, heat transfer analysis and applications. *Applied Thermal Engineering*. 2003;23(3):251-283. DOI: 10.1016/S1359-4311(02)00192-8
- [9] Jahns E. Microencapsulated phase change material. Paper presented at the 4th workshop IEA ECES Benediktbeuern Germany; October 1999. 28-29
- [10] Mehling H. Latent heat storage with a PCM-graphite composite material: Experimental results from the first test store. In: 6th Workshop of IEA Annex 10 Phase Change Materials and Chemical Reactions for Thermal Energy Storage; Stockholm. 2000
- [11] Narayanan SS, Kardam A, Kumar V, Bhardwaj N, Madhwal D, Shukla P, et al. Development of sunlight-driven eutectic phase change material nanocomposite for applications in solar water heating. *Resource-Efficient Technologies*. 2017;3(3):272-279. DOI: 10.1016/j.reffit.2016.12.004
- [12] Vijay Padmaraju SA, Vignes M, Nallusamy N. Comparative study of sensible and latent heat storage systems integrated with solar water heating unit. *Renewable Energy and Power Quality Journal*. 2008;1(06):55-60. DOI: 10.24084/repqj06.218
- [13] Lu Y, Roskilly AP, Wang Y, Wang L. Study of a novel dual-source chemisorption power generation system using scroll expander. *Energy Procedia*. 2017;105:921-926. DOI: 10.1016/j.egypro.2017.03.417
- [14] Fopah Lele A. State-of-Art of thermochemical heat storage systems. 2016. pp. 15-58. DOI: 10.1007/978-3-319-41228-3_2

- [15] Regin AF, Solanki SC, Saini JS. Heat transfer characteristics of thermal energy storage system using PCM capsules: A review. *Renewable and Sustainable Energy Reviews*. 2008;**12**(9):2438-2458. DOI: 10.1016/j.rser.2007.06.009
- [16] Lane GA, Shamsundar N. Solar heat storage: Latent heat materials, Vol. I: Background and scientific principles. *Journal of Solar Energy Engineering*. 1983;**105**(4):467. DOI: 10.1115/1.3266412.
- [17] Zeinelabdein R, Omer S, Gan G. Critical review of latent heat storage systems for free cooling in buildings. *Renewable and Sustainable Energy Reviews*. 2018;**82**:2843-2868. DOI: 10.1016/j.rser.2017.10.046
- [18] Chandra D, Ding W, Lynch RA, Tomlinson JJ. Phase transitions in “plastic crystals”. *Journal of the Less-Common Metals*. 1991;**168**(1):159-167. DOI: 10.1016/0022-5088(91)90042-3
- [19] Vats G, Vaish R. Phase change materials selection for latent heat thermal energy storage systems (LHTESS): An industrial engineering initiative towards materials science. *Advanced Science Focus*. 2014;**2**(2): 140-147. DOI: 10.1166/asfo.2014.1091
- [20] Abhat A. Low temperature latent heat thermal energy storage: Heat storage materials. *Solar Energy*. 1983;**30**(4):313-332. DOI: 10.1016/0038-092x(83)90186-x
- [21] Kitajgorodskij AI. L'empaquetage de molécules longues. *Acta Crystallographica*. 1957;**10**:802
- [22] Muller A. An X-ray investigation of normal paraffins near their melting points. *Proceedings of the Royal Society A: Mathematical, Physical and Engineering Sciences*. 1932;**138**(836):514-530. DOI: 10.1098/rspa.1932.0200
- [23] Dirand M, Bouroukba M, Chevallier V, Petitjean D, Behar E, Ruffier-Meray V. Normal alkanes, multialkane synthetic model mixtures, and real petroleum waxes: Crystallographic structures, thermodynamic properties, and crystallization. *Journal of Chemical & Engineering Data*. 2002;**47**(2): 115-143. DOI: 10.1021/je0100084
- [24] Mukherjee PK, Dey S. Simple Landau model of the liquid-RII-RI rotator phases of alkanes. *Journal of Modern Physics*. 2012;**03**(01):80-84. DOI: 10.4236/jmp.2012.31012
- [25] Mondal S. Phase change materials for smart textiles—An overview. *Applied Thermal Engineering*. 2008;**28**(11-12):1536-1550. DOI: 10.1016/j.applthermaleng.2007.08.009
- [26] Karkri M, Lachheb M, Gossard D, Ben Nasrallah S, AlMaadeed MA. Improvement of thermal conductivity of paraffin by adding expanded graphite. *Journal of Composite Materials*. 2015;**50**(19):2589-2601. DOI: 10.1177/0021998315612535
- [27] Pokhrel R, González JE, Hight T, Adalsteinsson T. Analysis and design of a paraffin/graphite composite PCM integrated in a thermal storage unit. *ASME 2008 2nd International Conference on Energy Sustainability*. 2008;**2**:621-629. DOI: 10.1115/es2008-54043
- [28] Mondieig D, Rajabalee F, Metivaud V, Oonk HAJ, Cuevas-Diarte MA. n-Alkane binary molecular alloys. *Chemistry of Materials*. 2004;**16**(5): 786-798. DOI: 10.1021/cm031169p
- [29] Kravchenko V. The eutectics and solid solutions of paraffins. *Acta Physicochimica URSS*. 1946;**21**:335-344
- [30] Agafonov IA, Garkushin IK, Miftakhov TT. Patterns of phase diagram changes in series of n-alkane

binary system. *Zhurnal Fizicheskoi Khimii*. 1999;**73**(5):681-685

[31] He B, Setterwall F. Technical grade paraffin waxes as phase change materials for cool thermal storage and cool storage systems capital cost estimation. *Energy Conversion and Management*. 2002;**43**(13):1709-1723. DOI: 10.1016/S019689040100005X

[32] Farid MM, Khudhair AM, Razack SAK, Al-Hallaj S. A review on phase change energy storage: Materials and applications. *Energy Conversion and Management*. 2004;**45**(9-10):1597-1615. DOI: 10.1016/j.enconman.2003.09.015

[33] Sharma A, Tyagi VV, Chen CR, Buddhi D. Review on thermal energy storage with phase change materials and applications. *Renewable and Sustainable Energy Reviews*. 2009;**13**(2):318-345. DOI: 10.1016/j.rser.2007.10.005

[34] Xie N, Huang Z, Luo Z, Gao X, Fang Y, Zhang Z. Inorganic salt hydrate for thermal energy storage. *Applied Sciences*. 2017;**7**(12):1317. DOI: 10.3390/app7121317

[35] Dannemand M, Johansen JB, Furbo S. Solidification behavior and thermal conductivity of bulk sodium acetate trihydrate composites with thickening agents and graphite. *Solar Energy Materials & Solar Cells*. 2016;**145**:287-295. DOI: 10.1016/j.solmat.2015.10.038

[36] De Paola M, Arcuri N, Calabrò V, De Simone M. Thermal and stability investigation of phase change material dispersions for thermal energy storage by T-history and optical methods. *Energies*. 2017;**10**(3):354. DOI: 10.3390/en10030354

[37] Lv P, Liu C, Rao Z. Review on clay mineral-based form-stable phase change materials: Preparation, characterization and applications. *Renewable and Sustainable Energy Reviews*. 2017;**68**:707-726. DOI: 10.1016/j.rser.2016.10.014

[38] Sutjahja IM, A U SR, Kurniati N, Pallitine ID, Kurnia D. The role of chemical additives to the phase change process of $\text{CaCl}_2 \cdot 6\text{H}_2\text{O}$ to optimize its performance as latent heat energy storage system. *Journal of Physics Conference Series*. 2016;**739**:012064. DOI: 10.1088/1742-6596/739/1/012064

[39] Espeau P, Roblès L, Mondieig D, Haget Y, Cuevas-Diarte MA, Oonk HAJ. Mise au point sur le comportement énergétique et cristallographique des n-alcanes. *Journal de Chimie Physique et de Physicochimie Biologique*. 1996;**93**:1217-1238. DOI: 10.1051/jcp/1996931217

[40] Barbillon P, Schuffenecker L, Dellacherie J, Balesdent D, Dirand M. Variation d'enthalpie subie de 260 K à 340 K par les n-paraffines, comprises entre l'octadécane ($n\text{-C}_{18}$) et l'hexacosane ($n\text{-C}_{26}$). *Journal de Chimie Physique et de Physicochimie Biologique*. 1991;**88**:91-113. DOI: 10.1051/jcp/1991880091

[41] Metivaud V, Rajabalee F, Oonk HAJ, Mondieig D, Haget Y. Complete determination of the solid (RI)-liquid equilibria of four consecutive n-alkane ternary systems in the range $\text{C}_{14}\text{H}_{30}$ - $\text{C}_{21}\text{H}_{44}$ using only binary data. *Canadian Journal of Chemistry*. 1999;**77**(3):332-339. DOI: 10.1139/v99-004

[42] Rajabalee F, Métivaud V, Mondieig D, Haget Y, Cuevas-Diarte MA. New insights on the crystalline forms in binary systems of n-alkanes: Characterization of the solid ordered phases in the phase diagram tricosane + pentacosane. *Journal of Materials Research*. 1999;**14**(06):2644-2654. DOI: 10.1557/jmr.1999.0354

[43] van Miltenburg JC, Oonk HAJ, Metivaud V. Heat capacities and derived thermodynamic functions of n-nonadecane and n-eicosane between 10 K and 390 K. *Journal of Chemical &*

Engineering Data. 1999;**44**(4):715-720.
DOI: 10.1021/je980231+

[44] Salaün F, Devaux E, Bourbigot S, Rumeau P. Development of phase change materials in clothing part I: Formulation of microencapsulated phase change. Textile Research Journal. 2010;**80**(3):195-205. DOI: 10.1177/0040517509093436

[45] Shim H, McCullough EA, Jones BW. Using phase change materials in clothing. Textile Research Journal. 2001;**71**(6):495-502. DOI: 10.1177/004051750107100605